

# Selective dimerization by a radical chain reaction in $\gamma$ -irradiated crystals of 1,3-bis(3-acetoxyprop-1-ynyl)-4-methoxy-6-methylbenzene

PERKIN  
2

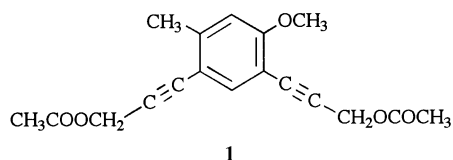
Yukio Yamamoto,<sup>\*,a</sup> Takashi Ueda,<sup>a</sup> Nobuko Kanehisa,<sup>b</sup> Keiichi Miyawaki,<sup>a</sup> Yoshio Takai,<sup>a</sup> Seiichi Tagawa,<sup>a</sup> Masami Sawada<sup>a</sup> and Yasushi Kai<sup>b</sup>

<sup>a</sup> The Institute of Scientific and Industrial Research, Osaka University, 8-1 Mihogaoka, Ibaraki, Osaka 567, Japan

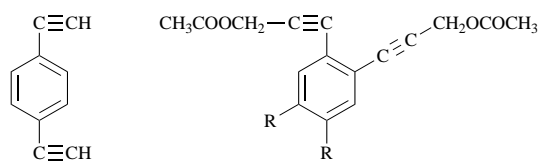
<sup>b</sup> Department of Applied Chemistry, Faculty of Engineering, Osaka University, 2-1 Yamadaoka, Suita, Osaka 565, Japan

A single dimer is formed by a radical chain reaction upon  $\gamma$ -irradiation of 1,3-bis(3-acetoxyprop-1-ynyl)-4-methoxy-6-methylbenzene (**1**) crystals, sealed in a glass ampoule under vacuum at room temperature. The dimerization is initiated by the addition of the prop-2-ynyl-type radical attached at the 1-position of the benzene ring to the  $\beta$ -carbon of the triple bond attached at the 3-position of the benzene ring. The resulting vinyl radical undergoes H-abstraction from the prop-2-ynyl methylene of the 3-acetoxyprop-1-ynyl group attached at the 1-position resulting in a chain reaction. The dimerization proceeds after the  $\gamma$ -irradiation is stopped. The kinetic chain length of the dimerization may be more than  $2 \times 10^3$ . Such an exclusive formation of a dimeric product by the  $\gamma$ -irradiation was observed neither for benzene solutions of **1** nor for crystals of other disubstituted bis(3-acetoxyprop-1-ynyl)benzenes. The crystal structure of **1** is responsible for the selective dimerization by the chain reaction. A mechanism for the chain reaction is proposed on the basis of the crystal structure.

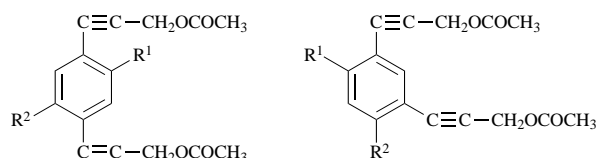
This paper is concerned with a unique dimerization occurring in  $\gamma$ -irradiated crystals of 1,3-bis(3-acetoxyprop-1-ynyl)-4-methoxy-6-methylbenzene **1**. Numerous studies have been pub-



lished on the solid-state polymerization of acetylenic compounds. Most of them have been undertaken for diacetylenes having a wide variety of substituents.<sup>1-3</sup> Crystals of 1,4-diethynyl-naphthalene, 1,4-diethynylbenzene **2** and their



**3** R = CH<sub>3</sub>  
**5** R = OCH<sub>3</sub>



**10** R<sup>1</sup> = OCH<sub>3</sub>, R<sup>2</sup> = CH<sub>3</sub>

**6** R<sup>1</sup> = R<sup>2</sup> = CH<sub>3</sub>  
**7** R<sup>1</sup> = R<sup>2</sup> = OCH<sub>3</sub>  
**8** R<sup>1</sup> = Et, R<sup>2</sup> = OCH<sub>3</sub>  
**9** R<sup>1</sup> = CH<sub>3</sub>, R<sup>2</sup> = OCH<sub>2</sub>CH<sub>3</sub>

analogues have also been reported to polymerize upon UV irradiation.<sup>4,5</sup> One of the ethynyl groups participates in the

polymerization resulting in a polyene polymer backbone. We have previously reported the polymerization occurring in the  $\gamma$ -irradiated crystals of diethynylbenzene derivatives such as **2**, 1,2-bis(3-acetoxyprop-1-ynyl)-4,5-dimethylbenzene **3**, 1,4-bis(3-acetoxyprop-1-ynyl)-2,6-dimethylbenzene **4** and 1,2-bis(3-acetoxyprop-1-ynyl)-4,5-dimethoxybenzene **5**.<sup>6</sup> The crystal structures of these monomers were determined by means of X-ray diffraction.<sup>7</sup> The polymer yield decreases in the order **3** > **2** > **4**. No polymer is produced in the irradiated crystals of **5**. The reactivities of the crystals are correlated to the distances between the acetylenic carbons taking part in bond formation for the head-to-tail addition polymerization in the crystals. The carbon-carbon distances are 3.628, 3.717, 3.987 and >5 Å for **3**, **2**, **4** and **5**, respectively. The arrangement of the triple bonds in the crystals of **5** has also revealed that the successive addition reaction of the triple bonds is impossible.<sup>7</sup>

It has been shown in our previous study that the crystal structures of diethynylbenzene derivatives are strongly affected by the nature of the substituents and their positions in the aromatic ring.<sup>7</sup> The study on the reactivities of  $\gamma$ -irradiated crystals has been extended to several other bis(3-acetoxyprop-1-ynyl)benzene derivatives. It was found that the crystals of **1** have an extremely high reactivity toward  $\gamma$ -irradiation to give exclusively a single dimer by a chain reaction. The reactivities of the  $\gamma$ -irradiated crystals were also tested for the analogues of **1**, such as 1,3-bis(3-acetoxyprop-1-ynyl)-4,6-dimethylbenzene **6**, 1,3-bis(3-acetoxyprop-1-ynyl)-4,6-dimethoxybenzene **7**, 1,3-bis(3-acetoxyprop-1-ynyl)-4-methoxy-6-ethylbenzene **8**, 1,3-bis(3-acetoxyprop-1-ynyl)-4-ethoxy-6-methylbenzene **9** and 1,4-bis(3-acetoxyprop-1-ynyl)-2-methoxy-5-methylbenzene **10**. Selective dimerization was not observed for these diethynylbenzene derivatives. The crystal structure is responsible for the unique reaction of **1**.

## Experimental

### Materials

The monomer **1** was prepared by the coupling of 1,3-diiodo-4-methoxy-6-methylbenzene and 3-acetoxyprop-1-yne by the literature method<sup>8</sup> and was purified by repeated recrystallization

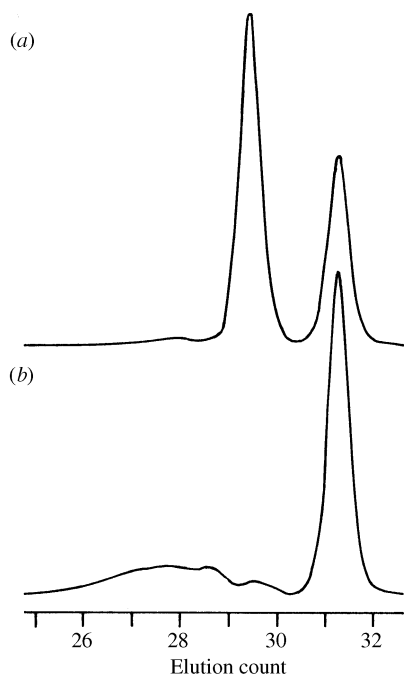


**Fig. 1** Gel permeation chromatograms (a) of the crystals of **1**, irradiated for 24 h, and (b) of the benzene solution of  $0.5 \text{ mol dm}^{-3}$  **1**, irradiated for 48 h and freed of solvent by freeze-drying

from benzene–hexane mixtures: mp  $74\text{--}75^\circ\text{C}$ ; mass spectrum,  $m/z$  314. 1,3-Diiodo-4-methoxy-6-methylbenzene was obtained by the direct iodination of 3-methylanisole using iodine and periodic acid dihydrate in a mixed solvent consisting of acetic acid, water and sulfuric acid.<sup>9</sup> 3-Acetoxyprop-1-yne was prepared from prop-2-ynyl alcohol and acetic anhydride by using sulfuric acid. The crystals of **6** (mp  $39^\circ\text{C}$ ), **7** (mp  $137\text{--}138^\circ\text{C}$ ), **8** (mp  $42\text{--}43^\circ\text{C}$ ), **9** (mp  $48^\circ\text{C}$ ), and **10** ( $105\text{--}106^\circ\text{C}$ ) were obtained in the same manner.

#### Irradiation and product analysis

The monomer crystals were sealed in a Pyrex tube under vacuum and were irradiated at room temperature with  $\gamma$ -rays from a  $^{60}\text{Co}$  source at a dose rate of  $4.5 \times 10^3 \text{ Gy h}^{-1}$  ( $1 \text{ Gy} = 1 \text{ J kg}^{-1}$ ). The molecular mass distribution of the irradiated crystals was measured with a gel permeation chromatograph (Toyo Soda HLC 802 A) in tetrahydrofuran. Two 61 cm TSK-Gel G2000H8 and G-4000H8 columns connected in series were used for the measurement. The isolation of the dimer and the determination of its yield were carried out using a liquid chromatograph (JASCO 800 system; silica-gel column, chloroform).  $^1\text{H}$  NMR spectra were recorded on a 360 MHz NMR spectrometer (Bruker, WM-360) in  $\text{CDCl}_3$  with  $\text{SiMe}_4$  as an internal standard. The benzene solutions of **1**, **3** and **5** ( $0.5 \text{ mol dm}^{-3}$ ) were degassed by the freeze–thaw method (repeated three times) and sealed. The ampoules of the solutions were irradiated with  $\gamma$ -rays in the same manner as those of the crystals.

#### X-Ray structure determination

X-Ray diffraction data were measured on a Rigaku AFC-5R diffractometer with  $\beta$ -filtered  $\text{Cu-K}\alpha$  radiation ( $\lambda = 1.5418 \text{ \AA}$ ). A total of 2578 reflections for **1** were collected by the  $\theta$ - $2\theta$  scan technique up to  $2\theta = 120^\circ$ . The crystal structure was solved by the direct method and refined by full-matrix least-squares analysis using the 2083 observed reflections [ $I_o > 3\sigma(I_o)$ ] with  $w = 1/\sigma^2(F_o)$ . The refinement proceeded by assuming anisotropic thermal parameters for non-hydrogen atoms and isotropic ones for hydrogen atoms. The final discrepancy factors  $R$  and  $R_w$  are 0.060 and 0.055, respectively.

#### Crystal data

$\text{C}_{18}\text{H}_{18}\text{O}_5$ , **1**,  $M = 314.34$ , monoclinic, space group  $P2_1/n$ ,

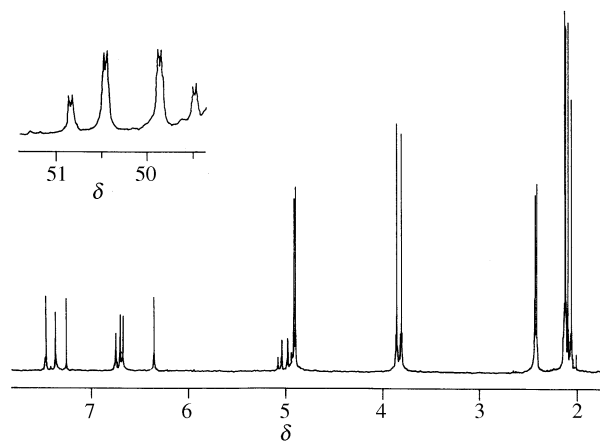


**Fig. 2** NMR spectrum of the dimer

$a = 11.627(1)$ ,  $b = 19.119(1)$ ,  $c = 7.540(1) \text{ \AA}$ ,  $\beta = 96.33(1)^\circ$ ,  $V = 1665.9(2) \text{ \AA}^3$ ,  $Z = 4$ ,  $D_c = 1.253 \text{ g cm}^{-3}$ ,  $F(000) = 664$ ,  $\mu(\text{Cu-K}\alpha) = 7.6 \text{ cm}^{-1}$ ,  $T = 295 \text{ K}$ . Atomic coordinates, bond lengths and angles, and thermal parameters have been deposited at the Cambridge Crystallographic Data Centre (CCDC). For details of the deposition scheme, see 'Instructions for Authors', *J. Chem. Soc., Perkin Trans. 2*, 1997, Issue 1. Any request to the CCDC for this material should quote the full literature citation and the reference number 188/58.

## Results and discussion

#### Dimerization in irradiated crystals

Fig. 1 shows the gel permeation chromatograms of the irradiated crystals and  $0.5 \text{ mol dm}^{-3}$  benzene solution of **1**, which were irradiated for 24 and 48 h, respectively. The irradiated benzene solution was freed of solvent by freeze-drying before submitting to chromatography. The peaks at the elution counts of 29.3 and 31.3 in the chromatograms of the irradiated crystals are assigned to the dimer and the monomer, respectively. No higher molecular mass products were detected in the crystals irradiated within 24 h. Prolonged irradiation resulted in the formation of polymeric products probably produced from the dimer because of the high conversion into the dimer. On the other hand, when irradiated in benzene solution, polymeric products are formed without a remarkable formation of dimeric products. The polymerization in benzene solution was also examined for **3** and **5**, whose crystals have quite different reactivities upon  $\gamma$ -irradiation as described above.<sup>6</sup> The yields and the molecular mass distributions of the polymeric products from the benzene solutions of **3** and **5** were almost the same as those from the benzene solution of **1**. The reactivities of these diethynylbenzene derivatives in solution are considered to be similar as expected from the resemblance of the monomer structures.

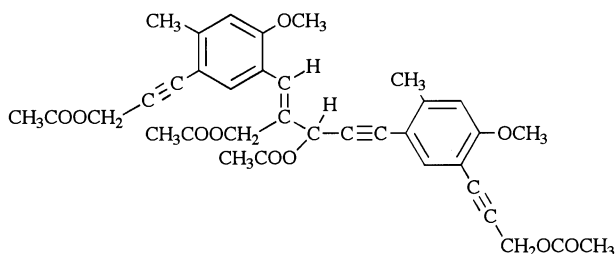
The dimer was isolated and characterized by using  $^1\text{H}$  NMR and mass spectrometry. The isolated dimer was a highly viscous liquid at room temperature. The NMR spectrum of the dimer is shown in Fig. 2. The NMR data are compared with those of **1** in Table 1. The signals at 6.36 and 6.76 ppm in the dimer spectrum must originate from  $\text{CHC}\equiv\text{C}$  and  $\text{CH}=\text{C}$ , respectively. Thus, the dimer is suggested to be produced by the addition of a prop-2-ynyl-type radical to a triple bond. Each signal of  $\text{CH}_3$ ,  $\text{CH}_3\text{O}$  and  $\text{ArH}$  in the monomer spectrum becomes two in the dimer spectrum. This means that a single dimer is selectively produced by the addition of the prop-2-ynyl-type radical to the triple bond, although four isomeric dimers could be formed from the unsymmetrically disubstituted bis(3-acetoxyprop-1-ynyl)benzene by the addition reaction of the 3-acetoxyprop-1-ynyl groups.

The two signals of  $-\text{CH}_2\text{C}\equiv\text{C}-$  of the monomer at 4.90 and 4.92 ppm remain in the dimer spectrum (4.91 and 4.92 ppm).

**Table 1**  $^1\text{H}$  NMR data for **1** and the dimer

Proton	<b>1</b> $\delta$ (m/z 314)	Dimer $\delta$ (m/z 628)
OCOCH <sub>3</sub>	2.11 (3 H, s) 2.12 (3 H, s)	2.07 (3 H, s), 2.10 (3 H, s) 2.13 (3 H, s), 2.14 (3 H, s)
ArCH <sub>3</sub>	2.42 (3 H, s)	2.42 (3 H, s), 2.44 (3 H, s)
ArOCH <sub>3</sub>	3.86 (3 H, s)	3.82 (3 H, s), 3.87 (3 H, s)
CH <sub>2</sub> C=C	4.90 (2 H, s) 4.92 (2 H, s)	4.91 (2 H, s) 4.92 (2 H, s)
CH <sub>2</sub> C=C		4.97 (1 H, dd <sup>a</sup> ), 5.06 (1 H, dd <sup>a</sup> )
CHC=C		6.36 (1 H, s)
HC=C		6.76 (1 H, br)
ArH	6.69 (1 H, s) 7.48 (1 H, s)	6.68 (1 H, s), 6.71 (1 H, s) 7.38 (1 H, s), 7.48 (1 H, s)

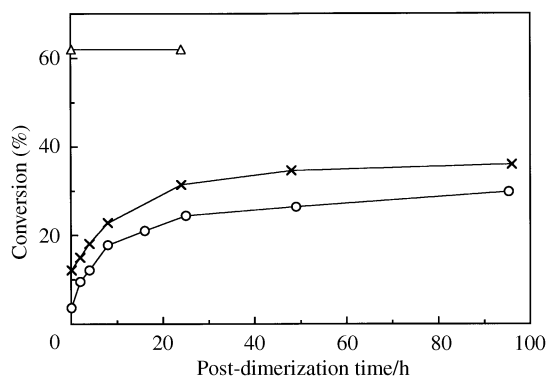
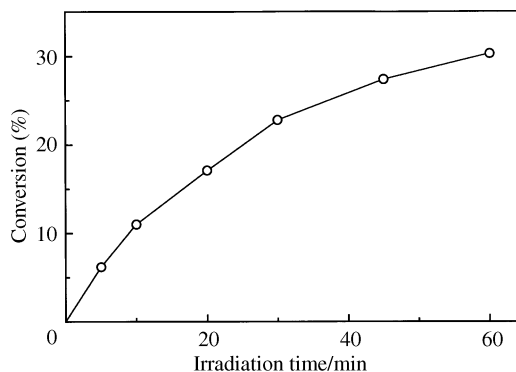
<sup>a</sup>  $J/\text{Hz}$  14.7 and 1.4.

**Fig. 3** Structure of the dimer

These signals in the dimer spectrum must originate from  $-\text{CH}_2\text{C}\equiv\text{C}-$  of the 3-acetoxyprop-1-ynyl groups not taking part in the addition reaction. This indicates that the 3-acetoxyprop-1-ynyl groups taking part in the addition reaction are those attached at the different positions of the aromatic ring of the monomer. All of the other signals in the monomer spectrum also seem to remain in the dimer spectrum. The signals in the dimer spectrum close to those in the monomer spectrum are considered to originate from the protons apart from the reaction sites. This also demonstrates that the addition reaction occurs between the 3-acetoxyprop-1-ynyl groups attached at the 1- and 3-positions but not between those attached at the same position of the aromatic ring of the monomer.

The signals at 6.69 and 7.48 ppm in the monomer spectrum are assigned to ArH at the 5- and 2-positions, H(5) and H(2), respectively. These signals are also observed in the dimer spectrum (6.68 and 7.48 ppm) and are assigned to ArH apart from the reaction site. The signals newly observed at 6.71 and 7.38 ppm in the dimer spectrum are considered to be derived from H(5) and H(2) of the monomer, respectively, which are close to the reaction site. Thus, it can be said that the signal of H(2) close to the reaction site is upfield shifted from the original monomer chemical shift (7.48 ppm) by 0.10 ppm, whereas that of H(5) is downfield shifted from the original monomer chemical shift (6.69 ppm) only by 0.02 ppm. A similar comparison is made for ArOCH<sub>3</sub> and ArCH<sub>3</sub> in the dimer spectrum. The signals of CH<sub>3</sub>O and CH<sub>3</sub> at 3.87 and 2.42 ppm must originate from the substituents apart from the reaction site. For ArOCH<sub>3</sub> and ArCH<sub>3</sub> close to the reaction site, it can be seen that the signal of ArOCH<sub>3</sub> of the dimer (3.82 ppm) is upfield shifted from the monomer chemical shift (3.86 ppm), whereas that of ArCH<sub>3</sub> of the dimer (2.44 ppm) is downfield shifted from the monomer chemical shift (2.42 ppm). These NMR data indicate that the triple bond of the 3-acetoxyprop-1-ynyl group attached at the 3-position is converted into the double bond by the addition reaction. Therefore, it can be concluded that the prop-2-ynyl-type radical attached at the 1-position adds to the triple bond. The structure of the dimer is shown in Fig. 3.

The NMR signals of  $-\text{CH}_2\text{C}=\text{C}<$ ,  $>\text{CHC}=\text{C}-$  and  $-\text{CH}=\text{C}<$  newly appear in the dimer spectrum at 4.95–5.09, 6.36 and 6.76 ppm, respectively. The signal of  $-\text{CH}_2\text{C}=\text{C}<$  is split into four peaks because of the presence of the asymmetric carbon

**Fig. 4** Dimer yields at different irradiation times vs. post-dimerization time:  $\circ$ , 30 min;  $\times$ , 60 min;  $\triangle$ , 24 h**Fig. 5** Dimer yield at the post-dimerization time of 24 h vs. irradiation time

attached at the same vinyl carbon. Each of the four peaks of  $-\text{CH}_2\text{C}=\text{C}<$  shows very small splitting, as shown in the inset of Fig. 2, due to the allyl coupling.

Fig. 4 shows the change in the dimer yield after the  $\gamma$ -irradiation. When irradiated for 30 or 60 min, the dimer yield increases greatly under storage in the sealed tubes without  $\gamma$ -irradiation, indicating an occurrence of post-dimerization. The  $G$  value of the dimer,  $G(\text{dimer})$ , was determined to be  $2.2 \times 10^3$  for the sample irradiated for 30 min and then kept in the sealed tube for 96 h; the symbol  $G$  means the number of molecules per 100 eV energy absorbed by the medium ( $100 \text{ eV} = 1.6 \times 10^{-17} \text{ J}$ ). This is the largest  $G(\text{dimer})$  value obtained at the shortest irradiation time and at the longest post-dimerization time among these experimental runs. Such a high  $G$  value shows that the dimer is produced by a chain reaction. The  $G$  values of radicals for irradiated aromatic compounds are rather smaller than unity.<sup>10</sup> Therefore, the kinetic chain length of the dimerization may be more than  $2 \times 10^3$ . On the other hand, when irradiated for 24 h, the dimer yield does not change after the irradiation is stopped. The  $G(\text{dimer})$  value calculated for the 24 h irradiated sample was 88. Fig. 5 shows the yield of the dimer at the storage time of 24 h plotted against irradiation time. The  $G(\text{dimer})$  value determined at the shortest irradiation time, 10 min, was  $2.4 \times 10^3$ , which is close to the value obtained above. When the sample irradiated for 30 min at room temperature was kept at  $0^\circ\text{C}$  for 96 h, the  $G(\text{dimer})$  was 740, which is smaller than the  $G(\text{dimer})$  for the room temperature storage. This means that the dimerization is an activated process.

The  $G$  values of the monomer consumption,  $G(-m)$ , for the polymerization of the  $\gamma$ -irradiated crystals of **3**, **2** and **4** are 17, 7.0 and 0.9, respectively.<sup>6</sup> The  $G(\text{dimer})$  value of **1** is much larger than the  $G(-m)$  values of **3**, **2** and **4**, demonstrating the unique specificity of the dimerization of the  $\gamma$ -irradiated crystals of **1**. The crystals of **6–10** were irradiated for 96 h and submitted to the gel permeation chromatograph. Small

**Table 2** Selected bond distances (Å) and angles (°) for the crystal structure of **1**<sup>a</sup>

O(1)–C(9)	1.461(5)	C(9)–O(1)–C(10)	116.8(4)
O(1)–C(10)	1.344(4)	C(14)–O(3)–C(15)	114.3(3)
O(2)–C(10)	1.193(4)	C(4)–O(5)–C(17)	118.2(3)
O(3)–C(14)	1.441(4)	C(2)–C(1)–C(6)	119.1(3)
O(3)–C(15)	1.339(4)	C(2)–C(1)–C(7)	119.1(3)
O(4)–C(15)	1.186(4)	C(6)–C(1)–C(7)	121.9(3)
O(5)–C(4)	1.364(3)	C(1)–C(2)–C(3)	122.5(3)
O(5)–C(17)	1.435(5)	C(2)–C(3)–C(4)	118.0(3)
C(1)–C(2)	1.383(4)	C(2)–C(3)–C(12)	120.3(3)
C(1)–C(6)	1.391(4)	C(4)–C(3)–C(12)	121.7(3)
C(1)–C(7)	1.444(4)	O(5)–C(4)–C(3)	115.5(3)
C(2)–C(3)	1.380(4)	O(5)–C(4)–C(5)	124.6(3)
C(3)–C(4)	1.401(4)	C(3)–C(4)–C(5)	119.9(3)
C(3)–C(12)	1.442(4)	C(4)–C(5)–C(6)	121.5(3)
C(4)–C(5)	1.377(4)	C(1)–C(6)–C(5)	119.0(3)
C(5)–C(6)	1.387(4)	C(1)–C(6)–C(18)	120.8(4)
C(6)–C(18)	1.506(5)	C(5)–C(6)–C(18)	120.2(4)
C(7)–C(8)	1.186(4)	C(1)–C(7)–C(8)	178.3(4)
C(8)–C(9)	1.460(5)	C(7)–C(8)–C(9)	177.4(4)
C(10)–C(11)	1.494(6)	O(1)–C(9)–C(8)	111.5(3)
C(12)–C(13)	1.178(4)	O(1)–C(10)–O(2)	122.4(4)
C(13)–C(14)	1.467(5)	O(1)–C(10)–C(11)	111.8(4)
C(15)–C(16)	1.481(6)	O(2)–C(10)–C(11)	125.9(5)
		C(3)–C(12)–C(13)	176.8(3)
		C(12)–C(13)–C(14)	176.2(3)
		O(3)–C(14)–C(13)	107.7(3)
		O(3)–C(15)–O(4)	121.9(3)
		O(3)–C(15)–C(16)	111.5(4)
		O(4)–C(15)–C(16)	126.6(5)

<sup>a</sup> For the numbering scheme of atoms, see Fig. 6.

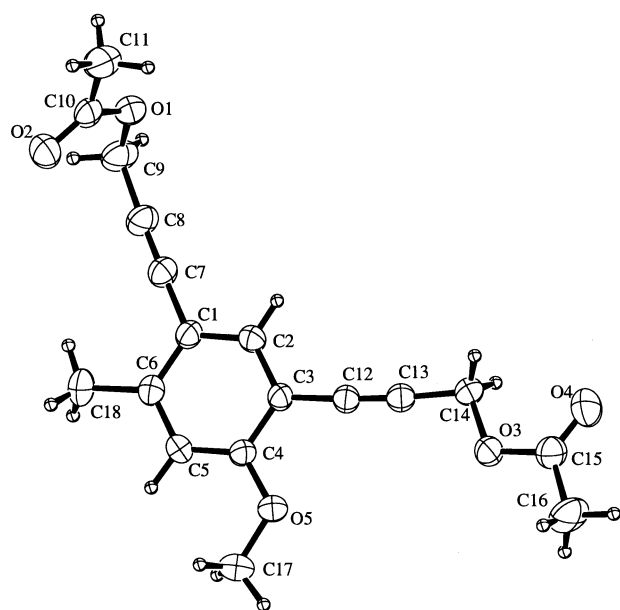


**Fig. 6** Molecular structure of **1** drawn by the thermal ellipsoids with 30% probability level

amounts of low molecular mass oligomers were detected for these monomer crystals. The reactivities of the crystals toward the  $\gamma$ -irradiation are considered to be as low as those of **4**.

The dimerization of the crystals of **1** is initiated by the addition of the prop-2-ynyl-type radical to the triple bond. The resulting vinyl radical exclusively abstracts a hydrogen from the prop-2-ynyl methylene group at the 3-position. It does not add to the triple bond to initiate the polymerization. Both the addition and the H-abstraction reactions are selective to give the dimer. Thus, the dimerization must be controlled by the molecular packing of the crystals.

#### Molecular and crystal structure

An X-ray analysis study has been done for the crystals of **1**. The

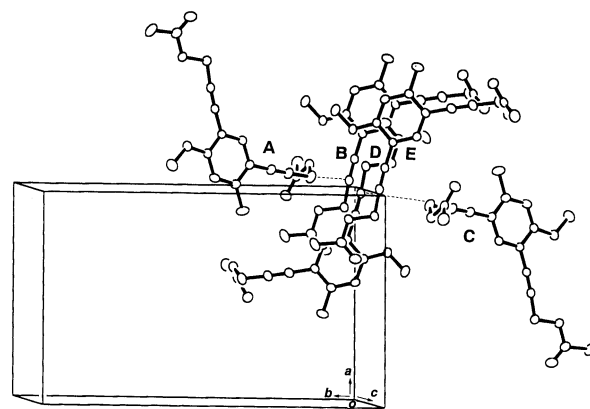


**Fig. 7** Crystal structure of **1**. The molecular labels, **A–E**, show the molecules drawn by the symmetry operations of: **A**:  $(1 + x, y, z)$ , **B**:  $(1.5 - x, -0.5 + y, 0.5 - z)$ , **C**:  $(1.5 - x, -0.5 + y, 1.5 - z)$ , **D**:  $(0.5 + x, 0.5 - y, -0.5 + z)$ , **E**:  $(1 - x, -y, 1 - z)$ . The broken lines are the closest intermolecular contacts of 3.539 Å between prop-2-ynyl methylene and  $\beta$ -carbon in triple bond.

molecular structure is shown in Fig. 6, and the selected bond lengths and angles are summarized in Table 2. The molecule has little conformational flexibility except the internal rotations around the C–CH<sub>2</sub> and CH<sub>2</sub>–O bonds in the 3-acetoxyprop-1-ynyl substituents. Because of the asymmetrical substituents on the phenyl ring, CH<sub>3</sub> on C6 and CH<sub>3</sub>O on C4, the internal rotations around the bonds are different from each other. The rotational angles around the C–CH<sub>2</sub> and CH<sub>2</sub>–O bonds,  $\phi_1$  and  $\phi_2$ , are  $-107$  and  $-78.2^\circ$  for the substituent on C1, respectively, and  $10^\circ$  and  $179.5^\circ$  for that on C3, respectively. Thus, the terminal acetoxy moiety of the former substituent deviates from the plane of the phenyl ring, and that of the latter locates on the plane. In the other words, 3-acetoxyprop-1-ynyl substituents are in the forms of bent and stretched arms on C1 and C3 positions, respectively. The different conformations of these substituents result in the different geometrical environments in the crystal lattice, which is the substantial factor to characterize the reactivity in the solid state.

Fig. 7 shows the crystal structure of **1**. The selective dimer formation is well interpreted in terms of the crystal structure. The methylene carbon of the 3-acetoxyprop-1-ynyl group at the 1-position is close to the  $\beta$ -carbon of the triple bond attached at the 3-position of the adjacent molecule. The intermolecular carbon–carbon distance is 3.539 Å, which is the shortest in those for the bond formation in the polymerization of **3**, **2** and **4**, shown above. Along the *c*-axis the adjacent molecules are stacked in the mode to insert their stretched 3-acetoxyprop-1-ynyl groups by turns.

#### Proposed chain mechanism for the dimerization

From the detailed examination of the crystal structure by the use of MOL-GGRAPH system, the following six steps are proposed for the selective dimerization by the chain reaction according to Fig. 8; the distances between the reacting carbons in the monomer crystal are shown in parentheses, and **A–F** denote the monomer molecules taking part in the dimerization steps. (1) The prop-2-ynyl-type radical of **A** adds to  $\beta$ -carbon of the triple bond of **B** (3.539 Å). (2) The resulting vinyl radical of **B** abstracts a hydrogen from the prop-2-ynyl methylene group of **C** (4.385 Å) and the first dimer molecule is formed from **A** and **B**. (3) The newly formed prop-2-ynyl-type radical of **C** adds to  $\beta$ -carbon of the triple bond of **D** (3.539 Å). (4) The resulting vinyl radical of **D** abstracts a hydrogen from the prop-2-ynyl methylene group of **E** (3.880 Å) and the second dimer molecule is formed from **C** and **D**. (5) The prop-2-ynyl-type radical of **E** abstracts a hydrogen from the prop-2-ynyl methylene group of **F** (3.704 Å). (6) The resulting prop-2-ynyl-type radical of **F** adds to  $\beta$ -carbon of the triple bond of **E** (3.539 Å) to initiate

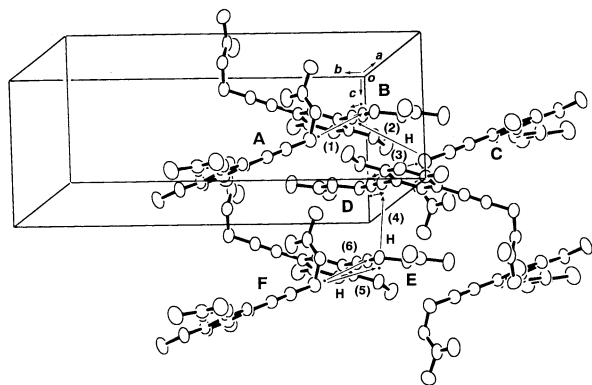


**Fig. 8** Chain reaction mechanism for the dimerization in the crystal of **1**. The crystal structure of this figure was obtained from Fig. 8 by the anticlockwise rotation of *ca.* 90° around the *b*-axis and translation of one unit cell along the *c*-axis towards the negative direction. The molecular labels correspond to those in Fig. 8, and the molecule **F** is equivalent to the molecule **A** translated by one unit cell along the *c*-axis. The stepwise mechanism in the text are shown in the figure by the numbers in parentheses.

the dimerization steps in the neighbouring unit cell. Each unit cell contains four monomer molecules to give two dimer molecules. The two-step H-abstractions, steps (4) and (5), were proposed instead of the direct H-abstraction from **F** to **D** because the carbon-carbon distance for the direct H-abstraction is 6.392 Å and is too long to occur. Thus, all the interatomic constants involved in the reaction mechanism are around 4 Å, which are quite reasonable for the occurrence of the dimerization by the chain reaction. It should be noted that radicals apart from reaction sites in crystals are long-lived and that the rate of the dimerization is rather low, as is shown by the occurrence of the post-dimerization (Fig. 4). On this basis, it seems reasonable to propose the selective dimerization processes involving the two-step H-abstractions.

For the formation of the single dimer with yields in an order of  $10^3$  per one radical to occur, the movement of the monomer molecules should be minimum during the addition and H-

abstraction processes. The MM2 calculations revealed that the approximate size and shape of the space occupied by the two monomer molecules or the dimer molecule do not change so drastically during the dimerization processes except a slight shrinkage in volume. This fact shows that the movement of the monomer molecules toward dimerization is not severely affected by the steric constraint of the adjacent molecules. It also indicates that the slight movement of the monomer molecules during the dimerization does not cause a destructive effect on the crystal structure which prevents the smooth propagation of the radical centre in the chain reaction mode.

### Acknowledgements

This work was partly supported by a Grant-in-Aid for Scientific Research on Priority Areas (Nos. 06242102, 08221219) from the Ministry of Education, Science and Culture, Japan.

### References

- 1 H. Basseler, *Adv. Polym. Sci.*, 1984, **63**, 1.
- 2 H. Sixl, *Adv. Polym. Sci.*, 1984, **63**, 49.
- 3 V. Enkelmann, *Adv. Polym. Sci.*, 1984, **63**, 91.
- 4 O. Rohde and G. Wegner, *Makromol. Chem.*, 1978, **179**, 1999.
- 5 O. Rohde and G. Wegner, *Makromol. Chem.*, 1978, **179**, 2013.
- 6 M. Hagihara, Y. Yamamoto, S. Takahashi and K. Hayashi, *Radiat. Phys. Chem.*, 1986, **28**, 165.
- 7 Y. Kai, A. Yamamoto, D. Xu, N. Kasai, M. Hagihara, Y. Yamamoto, S. Takahashi and K. Hayashi, *Makromol. Chem.*, 1987, **188**, 3047.
- 8 S. Takahashi, Y. Kuroyama, K. Sonogashira and N. Hagihara, *Synthesis*, **1980**, 627.
- 9 H. Suzuki, K. Nakamura and R. Goto, *Bull. Chem. Soc. Jpn.*, 1966, **39**, 128.
- 10 E. R. Klinshpont, *Organic Radiation Chemistry Handbook*, eds. V. K. Milinchuk and V. I. Tupikov, Ellis Horwood, Chichester, 1989, p. 34.

Paper 6/06715H  
Received 2nd October 1996  
Accepted 3rd December 1996